

Epigenetic memory of oxidative stress: does nephrlin exert its protective effects via Rac1?

Desmond D Mascarenhas^{1,2}
David N Herndon³
Istvan Arany⁴

¹Mayflower Organization for Research & Education, Sunnyvale, CA, ²Transporin, Inc., Sunnyvale, CA, ³Department of Surgery, The University of Texas Medical Branch, and Shriners Hospitals for Children, Galveston, TX, ⁴Department of Pediatrics, Division of Pediatric Nephrology, University of Mississippi Medical Center, Jackson, MS, USA

Aim: Nephrlin peptide, a designed inhibitor of Rictor complex (mTORC2), exerts pleiotropic protective effects in metabolic, xenobiotic and traumatic stress models. Stress can generate enduring epigenetic changes in gene function. In this work we examine the possibility that nephrlin treatment protects against acute and enduring global changes in oxidative metabolism, with a focus on the Rictor-complex-mediated activation of Rac1, a subunit of NADPH oxidase (Nox) via PKCs, Prex1 and p66shc.

Methods: Given the wide range of animal models in which nephrlin peptide has previously demonstrated effectiveness *in vivo*, we chose three different experimental systems for this investigation: dermal fibroblasts, renal proximal tubule epithelial cells (PTECs), and kidney tissue and urine from an animal model of burn trauma in which nephrlin was previously shown to prevent loss of kidney function.

Results: (1) Nephrlin protects dermal fibroblasts from loss of viability and collagen synthesis after ultraviolet A (UV-A) or H₂O₂ insult. (2) Nephrlin reduces reactive oxygen species (ROS) formation by H₂O₂-treated (PTECs) with or without nicotine pretreatment. Using RNA arrays and pathway analysis we demonstrate that nicotine and H₂O₂-treated PTECs specifically induced Rac1 gene networks in these cells. (3) Using kidney tissue and urine from the burn trauma model we demonstrate significant elevations of [a] 8-aminoprostane in urine; [b] kidney tissue histone modification and DNA methylation; and [c] post-transcriptional phosphorylation events consistent with Rac1 activation in kidney tissue.

Conclusion: Nephrlin protects against oxidative stress, possibly by modulating the activation of Rac1.

Keywords: nephrlin, epigenetic, Rac1, burn injury, Rictor, 8-isoprostane

Introduction

Organisms respond to stress with enduring changes in metabolism, some of which can be epigenetically transmitted to offspring.^{1,2} It is thought that such persistent changes may involve DNA and histone modification.^{3,4}

Nephrlin is a 40-mer peptide designed as an inhibitor of Rictor complex (also known as mammalian target of rapamycin complex 2, mTORC2). The protective effects of nephrlin have been documented in animal models of metabolic, xenobiotic and traumatic stress.⁵⁻⁸ In previous studies we showed that nephrlin exerts pleiotropic protective effects in a model of severe burn injury, modulating persistent changes in inflammation and sepsis, loss of lean body mass, glycemic control, kidney function and wound healing.^{7,8} The mechanism(s) by which nephrlin peptide exerts its protective effects have not been fully elucidated. Because of the remarkable range of

Correspondence: Desmond Mascarenhas
Mayflower Organization for Research and Education
428 Oakmead Pkwy, Sunnyvale, CA
94085, USA.
Tel: +1 408 523 6279
E-mail: desmond@transporin.com

efficacy of neprilisin in many disease models we decided to investigate whether oxidative stress might play a role in the action of neprilisin. We chose to investigate this question in three distinct experimental systems, two in vitro and one in vivo, as individual test systems may exhibit idiosyncrasies.

The pathways by which cells respond epigenetically to stress insult are not well understood. In this work we investigate the hypothesis that neprilisin exerts its pleiotropic protective effects by modulating epigenetic and post-transcriptional changes that conspire to stimulate oxidative stress.

Rho-family GTPases are activated by a variety of extracellular signals. Some well described targets include RhoA (Ras homolog gene family, member A), Cdc42 (cell division control protein 42), and Rac1 (Ras-related C3 botulinum toxin substrate 1). Rac1, an obligate subunit of activated NADPH oxidase, plays a central role in oxidative metabolism in skin and other tissues. Some substrates activated by Rictor complex, such as Prex1/2 and PKC-alpha, may play a role in Rac1 and ERK activation.

Reactive oxygen species (ROS) play an important role in skin cells. UV-A radiation, in particular, is thought to stimulate oxidative damage.^{9,10} Nicotine pre-exposure, especially in combination with hydrogen peroxide, enhances oxidative stress in renal proximal tubule cells, a finding that may be relevant to the clinical observation that smokers experience poorer outcomes in surgery and transplant settings. Activation of the key adaptor protein p66shc has been shown to play a role in this process.¹⁶ p66shc, which is activated by PKC-beta-2 (a substrate of Rictor complex) is known to activate Rac1.^{12,13}

In this work we show the protective effects of neprilisin on UV-A stress in dermal fibroblasts, and on H₂O₂-triggered oxidative stress in both dermal fibroblasts and nicotine-pre-exposed renal proximal tubule cells. We further investigate epigenetic and phosphorylation events in kidney tissues derived from a well-established rat scald model in which we previously demonstrated the protective effect of neprilisin on the pleiotropic effects of burn injury, including loss of kidney function.^{8,14} In this work we analyze frozen kidney tissue from these earlier studies to show that the action of neprilisin in vivo is consistent with its protective effects in vitro.

Materials and Methods

Reagents: Neprilisin peptide, a 40-mer peptide carrying a sequence derived from PRR5/Protor (the sequence is conserved in human, rat and mouse species) was synthesized by LifeTein Inc (Hillsborough, NJ, USA) and purified to >80% purity by HPLC. The design and characterization of

neprilisin have been previously described.⁵ The sequence of neprilisin peptide and the scrambled control sequence peptide are shown below:

Neprilisin: Ac-RGVTEDYLRLETLVQKVVSCKGFYK-KKQCRPSKGRKRGFCW-amide
Scrambled: Ac-RDLEGYRVLTTETLVQKVVSCKGFYK-KKQSRPSKGRKRGFSW-amide

BCA Protein Kit was from Pierce (Rockford, IL, USA). Antibodies for ELISAs were purchased from Santa Cruz Biotechnology (Santa Cruz, CA, USA) except for anti-phospho-p66shc-S36 and anti-collagen-I antibodies (Abcam, Cambridge, MA, USA). CellLytic M cell lysis reagent was obtained from Sigma (St. Louis, MO, USA). Urinary 8-iso-prostane ELISA assay kit was from Cayman Chemical (Ann Arbor, MI, USA).

Institutional Review Board Approval: All experiments reported in this study received formal approval from the Mayflower Organization for Research & Education Ethics/Institutional Review Board.

Cell Lines and Treatment: All assays were done in triplicate. Human HS27 skin fibroblasts were purchased from ATCC (Manassas, VA, USA) and grown at 37°C in DMEM+10% FBS and penicillin/streptomycin to log phase, then seeded in 96-well flat-bottom plates at 8,000 cells/well. After 24 hr incubation cells were treated with 10 uM H₂O₂ in PBS for 2 hrs, or UV irradiation as described.¹⁵ After insult, the cells were washed and fresh cell culture medium was added along with 20 ug/ml peptide, or buffer control. Cells were incubated for 5 days in a 37°C humidified 5% CO₂ incubator, supernatants were harvested for ELISA and cells were tested for viability (sulforhodamine B, SRB assay). The protocol from the supplier (GeneCopoeia, Inc., Rockville, MD, USA) was followed. 50 uL/well of cold fixation solution was added and the cells were incubated at 4 °C for 1 hr. Cells were washed 5 times with distilled water and stained with 50 uL/well SRB stain at RT for 30 min, then washed four times to remove unbound dye. 50 uL solubilization buffer was added per well (5 min, agitation) and the plate was read at 560 nm using a Tecan M200 Plate Reader (Tecan Trading AG, Switzerland). PTECs (NRK52E) were purchased from ATCC and maintained in DMEM supplemented with 10% fetal bovine serum (Life Technologies, Grand Island, NY, USA). Some cells were pre-treated with 200 uM nicotine overnight prior to treatment with either 10 mg/ml neprilisin or scrambled peptide followed by H₂O₂.

Determination of intracellular ROS production. For determination of ROS production cells were grown in T25

flasks and pre-treated with 200 μ M nicotine as needed. After trypsinization, cells were counted and loaded with the oxidant-sensitive 2',7'-dichlorofluorescein-diacetate (100 mM, DCFDA; Life Technologies) as described elsewhere.¹¹ After 30 mins of incubation at 37°C the dye was washed away with fresh HBSS and cells were placed in wells of a 96-well-plate (0.2×10^6 cell/well) and treated with 400 μ M H₂O₂. ROS production was determined by recording increase in fluorescence at 485nm_{exc}/530nm_{em} in 30-minute-intervals for up to 120 minutes in a plate reader (Fluorocount, Packard). ROS production was calculated as changes in fluorescence/30 minutes/ 0.2×10^6 cells and expressed as percentage of the corresponding untreated values.

Kidney tissue: Frozen rat left kidney tissue and rat urine were gifts from Dr. Celeste Finnerty at UTMB. The experiments from which these tissues were collected have been described in published reports.^{7,8} The rat scald burn model is a modified Walker-Mason model that induces inflammation and hypermetabolism in line with what severely burned patients experience.¹⁴ In the previously reported experiments, scalded animals showed significant reductions in eGFR that were reversed by nephrlin treatment. Group size for animal treatment groups was n=8 for saline-treated burn control (B) group and n=9 for nephrlin-treated burn group (N1, animals treated daily for 1 week post-burn). In addition, a sham control group (S) had four animals.

Cell extracts for ELISAs: Preparation of kidney tissue cell extracts for ELISAs was performed as previously described.⁶ Specific immunoreactivity was measured by ELISA according to the kit manufacturer's recommendations.

RNA extraction: 30-50 mg of tissue was homogenized in TRIzol® (Invitrogen, Carlsbad CA, USA) and RNA extracted according to the manufacturer's protocol. Linear Acrylamide (AMRESCO, Solon OH, USA) was added as a co-precipitant at a final concentration of 25 μ g/mL. Concentration and purity of the RNA was determined using the NanoDrop spectrophotometer (Thermo Scientific, Wilmington, DE, USA).

RNA microarray analysis. Total RNA was extracted from approximate 10×10^7 PTECs cultured either in the presence or absence of H₂O₂, or with both Nic+ H₂O₂. RNA samples were prepared for microarray analysis following Agilent's one-color microarray-based gene expression analysis Low Input Quick Amp Labeling v6.0. Briefly, an input of 100ng of high quality total RNA (RIN values from 9.8 to 10) was amplified to generate Cyanine-3 labeled cRNA. An amount of 1.65 μ g of labeled cRNA was hybridized on Agilent Rat Gene Expression Microarrays 4x44K (AMIDID 014879). Microarrays were scanned with the Agilent DNA Microarray

Scanner at a 3 μ m scan resolution. Data was processed with Agilent Feature Extraction 11.0.1.1 and quantile normalized with Agilent GeneSpring 12.0.

Quantitative PCR: Quantitative polymerase chain reaction (rt-qPCR) for gene transcripts were performed using RNA extracted from kidney tissue and expressed relative to transcripts of GAPDH, a housekeeping gene. The cDNA synthesis reaction was carried out using 1,000 nanograms of RNA in a final volume of 20 μ L following manufacturer's instructions (High-Capacity cDNA Reverse Transcription kit, Applied Biosystems, Foster City, CA, USA). qPCR was carried out with the Fast Real Time 7500 (Applied Biosystems). The final reaction volume was 20 μ L and contained: each primer at a final concentration of 200 nM, Power Sybr Green (Applied Biosystems) 1X and 2 μ L of template (dilution 1:4 of cDNA synthesis reaction). Samples and standards were run in triplicate. Primer sequences for detecting gene transcripts and control primers for glyceraldehyde-3-phosphate dehydrogenase (GAPDH) are proprietary. The thermo cycle conditions were as follows: one cycle at 50°C for 20 sec, one activation cycle at 95°C for 10 minutes, followed by 40 cycles of 15 seconds at 95°C, 45 seconds at 60°C. Melting curve analysis was carried out using the continuous method from the 7500 Software (Applied Biosystems) conducted at 60°C, with increments of 1°C for 15 seconds. Data analysis was carried out with 7500 Software (Applied Biosystems). The auto threshold and baseline options were used for the calculations of Ct values per well. The linear equation for the standard curve (i.e., for preparations containing known quantities of DNA) was then used to interpolate the numbers of copies present in unknown samples.

Statistical analysis: Probability values (*p* values) were computed using Student's *t*-test and expressed relative to sham group or saline-treated group.

Results

Effect of nephrlin on UV-treated skin fibroblasts

UV treatment of skin fibroblasts is known to generate enhanced oxidative stress.^{9,10} Dermal fibroblasts were irradiated with UV-A or treated with H₂O₂ and cultured as described in Methods. Cell viability (SRB assay) and collagen-I immunoreactivity in supernatants (ELISA) were measured. As shown in Figure 1, both UV-A and H₂O₂ treatments resulted in significantly reduced cell viability and collagen synthesis in fibroblasts. Co-treatment with 20 μ g/ml nephrlin reversed these deficits in all cases. In the non-

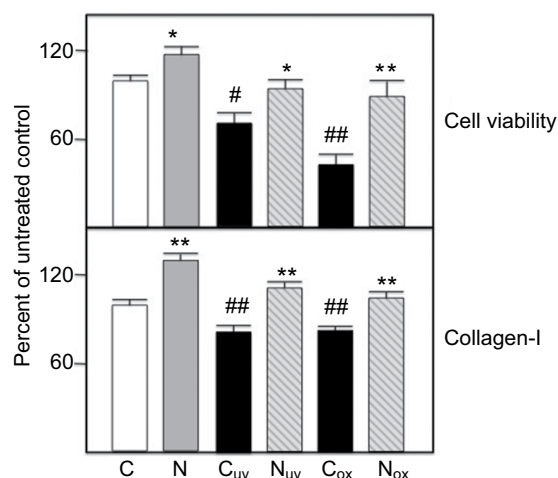


Figure 1. Fibroblasts were grown and challenged with either UV-A (_{UV} subscript) or H₂O₂ (_{ox} subscript) and cell viability and collagen I synthesis measured as described in Methods. Values are averages of triplicate assays and are expressed relative to control (=100). C=control untreated cells; N=20 ug/ml nephrlin peptide. *, **: p<0.05 and p<0.01 respectively, N versus C pairing; #, ##: p<0.05 and p<0.01 respectively, C_{UV} (or C_{ox}) versus C pairing.

irradiated control condition too, nephrlin treatment improved cell viability and collagen synthesis in fibroblasts.

Effect of nephrlin on renal PTECs treated with hydrogen peroxide

Treatment of cultured rat PTECs with H₂O₂ has been shown to generate p66shc-mediated ROS and oxidative stress. Pre-treatment with nicotine enhances these effects.¹⁶ We treated PTECs with H₂O₂ with or without nicotine pretreatment (Nic) as described in Methods. The results shown in Figure 2 show that H₂O₂ treatment significantly enhances cellular ROS in both cases. Co-treatment with 10 ug/ml nephrlin (but not a scrambled peptide control) at the time of H₂O₂ addition significantly reverses ROS generation.

RNA microarray analysis of genes induced by oxidative stress in PTECs.

Total RNA was extracted from PTECs cultured either in the presence or absence of H₂O₂, or with both Nic+H₂O₂. These RNAs were analyzed on Agilent Rat Gene Expression Microarrays 4x44K (AMDID 014879) as described in Methods. Of the 41,105 genes interrogated we identified 49 upregulated (>3-fold threshold) genes of known function, for which treatment with H₂O₂ alone was >30% over control, and treatment with the Nic+ H₂O₂ combination elevated expression an additional >30%. These genes are listed in Table 1. Of these, 29% are associated with Wnt and ERK signaling and 21% are associated with GTP-mediated signaling. Ingenuity Pathway software analysis (Palo Alto, CA,

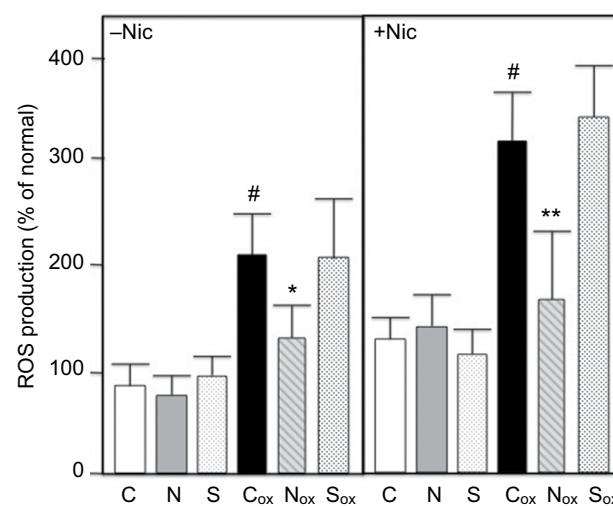


Figure 2. Renal PTECs were grown and challenged with H₂O₂ (_{ox} subscript) ± nicotine (Nic) and ROS generation measured as described in Methods. Values are averages of triplicate assays. C=control untreated cells; N=10 ug/ml nephrlin peptide; S=10 ug/ml scrambled peptide. *, **: p<0.05 and p<0.01 respectively, N (or S) versus C pairing; # = p<0.05 C_{ox} versus C.

USA) using a 3057 gene set in which changes of expression of any magnitude were reported, identified a Rac1/PKC/Prex1 cluster as the network generating a high score (=32) using their proprietary algorithms (Figure 3). These results, taken together, point to the possible involvement of Prex1, PKCs (both are known to be activated by Rictor complex) in Rac1-mediated effects on oxidative metabolism. Prex1 and (indirectly through p66shc) PKC-beta-2 are both known to activate Rac1.

Analysis of phosphorylation events in kidney tissue from animals treated with nephrlin in vivo

Frozen left kidney tissue slices from burned animals treated with saline or 4mg/kg/day nephrlin were analyzed by ELISA. These animals showed significantly reduced kidney function (eGFR) as a result of injury.⁸ The results of the ELISAs are shown in Figure 4. As suggested by the RNA array analysis, several key signaling molecules involved in the oxidative stress response were dramatically up-regulated by burn injury. These included the key molecules Rac1 and p66shc activated by phosphorylation at Ser71 and Ser36 respectively. In addition, PKC-beta (Ser660) and PKC-alpha (Ser657) were phosphorylated at cognate positions. Total PKC was also elevated. PKC-beta is responsible for activation of p66shc and PKC alpha is a key participant in ERK/Wnt pathway signaling. Nephrlin treatment significantly reversed all of these elevations in phosphorylation but not in total PKC-beta.

Table 1 RNA arrays. RNAs were extracted from cells and analyzed on Agilent Rat Gene Expression Microarrays 4x44K (AMIDID 014879) as described in Methods. Of 41,105 genes interrogated 49 upregulated (>3-fold threshold) genes of known function for which treatment with H₂O₂ alone was >30% over control and treatment with the Nic+ H₂O₂ combination elevated expression an additional >30% were identified.

ProbeName	GeneSymbol	GenbankAccession	GeneName	FOLD UPREG
A_44_P812665	Mypn	NM_001107628	myopalladin	9.3
A_42_P812805	Smoc2	NM_001106215	SPARC related modular calcium binding 2	8.4
A_44_P704258	En2	NM_001109214	engrailed homeobox 2	8.2
A_43_P12905	Bik	NM_053704	BCL2-interacting killer (apoptosis-inducing)	8.2
A_44_P288548	Prex1	NM_001135718	phosphatidylinositol-3,4,5-trisphosphate-dependent Rac exchange factor 1	8.0
A_44_P285988	Chrdl2	NM_001107537	chordin-like 2	7.6
A_44_P361951	Adssl1	XM_001072867	adenylosuccinate synthase like 1	7.2
A_44_P356161	Ppy	NM_012626	Pancreatic Polypeptide	7.1
A_43_P15474	Spef2	NM_022620	sperm flagellar 2	6.9
A_44_P572533	Cabyr	NM_001143893	calcium binding tyrosine-(Y)-phosphorylation regulated	5.8
A_44_P323349	Gria4	NM_017263	glutamate receptor, ionotropic, AMPA 4	5.7
A_42_P832832	Ckm	NM_012530	creatine kinase, muscle	5.6
A_44_P250467	Cd22	NM_001107503	CD22 molecule	5.2
A_42_P536266	Dnm3	XM_006250137	dynamin 3	5.2
A_44_P258225	Ly6h	NM_001134839	lymphocyte antigen 6 complex, locus H	5.2
A_44_P414340	Amelx	NM_019154	amelogenin, X-linked	5.0
A_44_P208532	Ido2	XM_006222273	indoleamine 2,3-dioxygenase 2	4.9
A_44_P145562	Dock2	XM_001068649	dedicator of cytokinesis 2	4.7
A_43_P13056	Il13Ora	NM_057193	interleukin 10 receptor, alpha	4.7
A_44_P665425	Rnfl65	NM_001164505	ring finger protein 165	4.5
A_44_P762053	Palld	XM_006253064	palladin, cytoskeletal associated Protein	4.4
A_44_P104630	Lat2	NM_173840	linker for activation of T cells family, member2	4.4
A_44_P236523	Hoxd10	NM_001107094	homeo box D10	4.4
A_44_P212521	Gzmf	NM_153466	granzyme F	4.3
A_44_P497282	Rab11fip4	NM_001107023	RAB11 family interacting protein 4 (class II)	4.3
A_44_P416899	Npy4r	NM_031581	neuropeptide V receptor V4	4.3
A_44_P1043302	Crb3	NM_001025661	crumbs homolog 3 (Drosophila)	4.3
A_44_P1036769	Matn1	NM_001006979	matrilin 1, cartilage matrix Protein	4.2
A_42_P841193	Ddit4l	NM_080399	DNA-damage-inducible transcript 4-like	4.2
A_44_P291071	Rora	NM_001106834	RAR-related orphan receptor A	4.2
A_43_P18101	Eif3	NM_001024768	E74-like factor 3	4.1
A_42_P525876	Erg	NM_133397	v-ets avian erythroblastosis virus E26 oncogene	4.0
A_44_P372305	Syn3	NM_017109	synapsin III	3.9
A_43_P19535	Mrgprb4	NM_001002287	MAS-related GPR, member B4	3.9
A_44_P520521	Scl7a2	NM_001107353	solute carrier family 17, member 2	3.8
A_44_P1001317	Nabp1	NM_001014216	nucleic acid binding protein 1	3.8
A_44_P555417	Hoga1	NM_001106355	4-hydroxy-2-oxoglutarate aldolase 1	3.7
A_44_P147156	Rbm47	NM_001005882	RNA binding motif protein 47	3.7
A_44_P199028	Dkk1	NM_001106350	dickkopf WNT signaling Pathway inhibitor 1	3.5
A_44_P144788	Mtmr12	XM_006232046	myotubularin related protein 12	3.5
A_43_P18793	Gfpt2	NM_001002819	glutamine-fructose-6-phosphate transaminase 2	3.4
A_44_P485948	Cux2	NM_0011271380	cut-like homeobox 2	3.3
A_44_P491864	Fgfl4	XM_006252526	fibroblast growth factor 14	3.1
A_44_P1020482	Nalcn	NM_153630	sodium leak channel, non-selective	3.0
A_42_P601961	Susd3	NM_001107341	sushi domain containing 3	3.0
A_44_P318628	Chrn2	NM_019297	cholinergic receptor, nicotinic, beta 2 (neuronal)	3.0
A_44_P1035007	Chrne	NM_017194	cholinergic receptor, nicotinic, epsilon (muscle)	3.0
A_44_P178498	B3gal5	NM_001105887	UDP-Gal:betaGlcNAc beta 1,3-galactosyltransferase, Polypeptide 5	3.0
A_44_P1048543	Ghrh	NM_031577	growth hormone releasing hormone	3.0

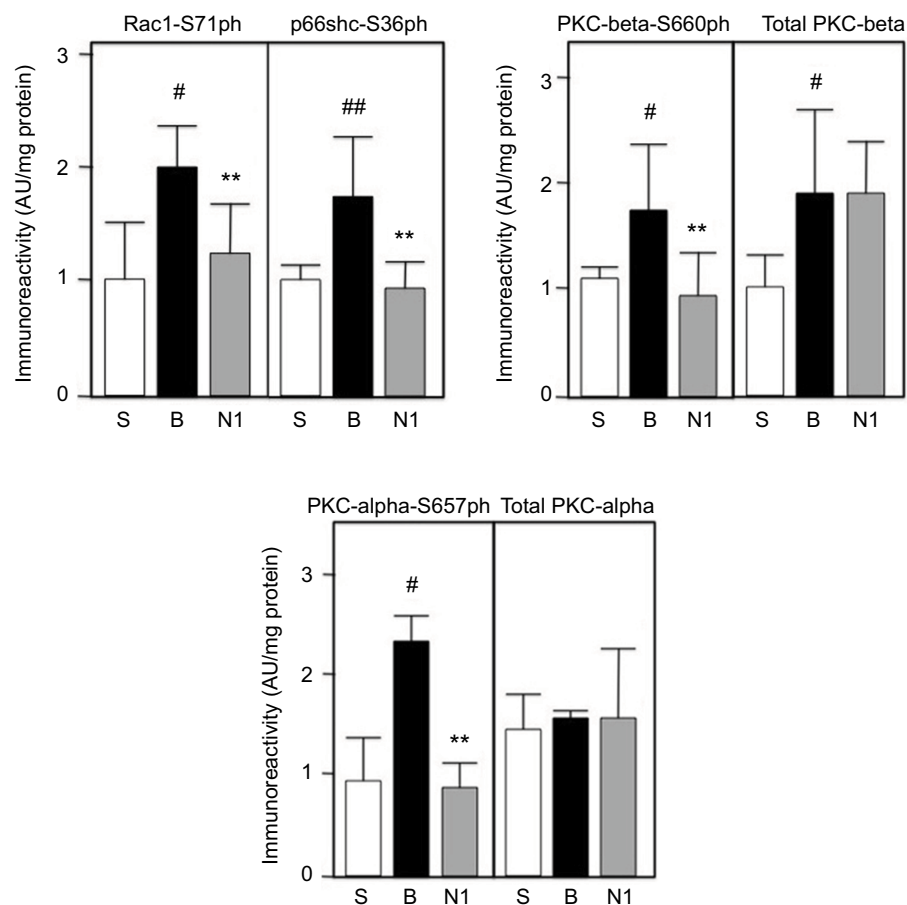


Figure 4. Kidney tissue extracts were prepared and analyzed by ELISA as described in Methods. S=sham group; B=burn+saline; N1=burn+4mg/kg/day SQ nephrilin for 1 week post-burn. ** $p<0.01$, N1 versus B; #, ##: $p<0.05$ and $p<0.01$, B versus S.

Abbreviation: AU, arbitrary units.

acetylation of histone 3 at residues Ly9/Lys14 are observed in saline-treated burned animals but not in the animals treated with nephrilin. This results suggests that enduring changes post-burn could be mediated, at least in part, by global changes in histone acetylation.

Methylation changes in Prex1 promoter region

We examined CpG islands in the region of DNA immediately upstream of the Prex1 gene. We focused on cytosine methylation in a CpG dinucleotide located at -601 (antisense strand) relative to the initiation codon. Figure 5d shows that methylation at this residue is dramatically reduced in burned animals, consistent with derepression of Prex1 gene expression. This reduction in methylation does not occur in animals treated with nephrilin.

Discussion

In this study we showed that nephrilin peptide specifically reverses the detrimental effects of oxidative stress in

(a) cultured fibroblasts (b) cultured PTECs and (c) tissues of rats that had experienced burn injury.

Nephrilin reverses the pronounced elevation of urinary 8-isoprostane in burned animals. Elevation of this marker in human subjects has been linked to increased NADPH oxidase activity in tissues.^{24,25} This result supports our hypothesis that nephrilin works by reversing the effects of oxidative stress.

Deficits in cell viability and collagen I synthesis in fibroblasts caused by UV-A or H₂O₂ insult are reversed by 20 ug/ml nephrilin. These insults are believed to increase oxidative stress in these cells and the reversal of their effects by nephrilin supports our hypothesis that nephrilin works by reversing the effects of oxidative stress.^{9,10} Protective effects are even seen in 'unstressed' controls, perhaps indicating the fact that all cultured cells are 'stressed' to some degree.

These results obtained with fibroblast cultures are also intriguing in the context of skin aging, which is believed to be at least partly driven by oxidative stress triggered by sun exposure.¹⁰ The addition of nephrilin peptide to skin via cosmetic formulations is a possible area of future inquiry,

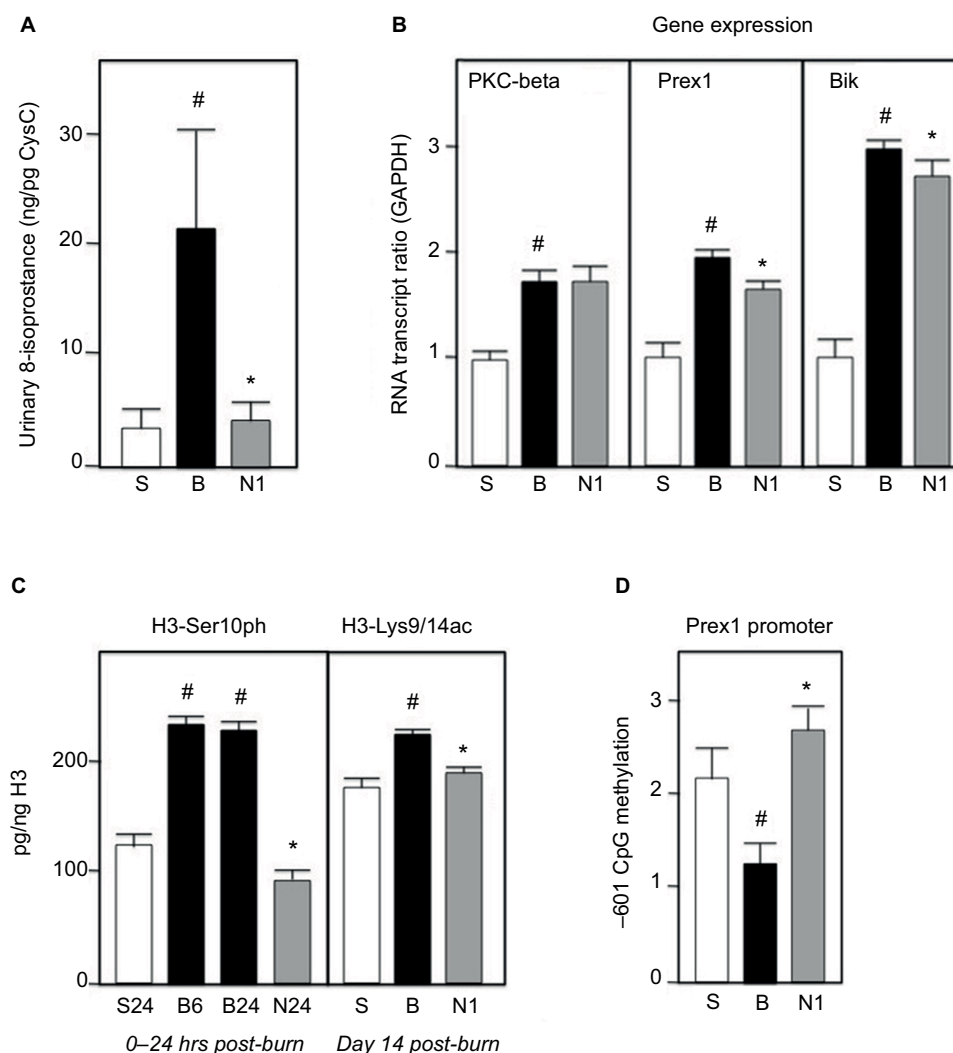


Figure 5. All extracts were prepared and assays performed as described in Methods. **(A)** Urine samples were assayed by ELISA and standardized against Cystatin C. **(B)** Gene transcripts were standardized versus GAPDH as standard. **(C)** Histone-3 phosphorylation and acetylation, as well as total histone-3, were determined by ELISA. Kidney tissues from 6 (B6=B group 6 hr) and 24 hours (S24, B24, N24) post-burn were assayed for phosphorylation, as early event. **(D)** CpG methylation is expressed in arbitrary units; each bar is an average of 4 animals. S=sham group; B=burn+saline; N1=burn+4mg/kg/day SQ nephrlin for 1 week post-burn. * $p < 0.05$, N1 versus B; # $p < 0.05$, B versus S.

though unaided penetration of the skin barrier by peptides is generally poor.

It was previously shown that long-term treatment with NIC exacerbates renal ischemia/reperfusion-dependent oxidative stress in vivo and oxidant (H_2O_2)-dependent ROS production in vitro.^{16,17} Here, we show that 10 $\mu\text{g/ml}$ nephrlin peptide but not a control (scrambled sequence) peptide protects PTECs by reducing nicotine-dependent ROS generation. Nephrlin peptide reverses the ROS-generating effects of H_2O_2 on renal PTECs with or without pre-exposure to nicotine. This result also supports our hypothesis that nephrlin works by reversing the effects of oxidative stress. Differential analysis of RNA array data from treated PTECs ($\pm H_2O_2$; \pm Nic;) further provided a gene list that supported the possible role of Rac1 and ROS generation.

Using rat kidney tissues previously harvested in a well-characterized burn model we were able to show burn stress-related (a) global elevations in histone-3 phosphorylation (Ser10) and acetylation (Ser9/14); (b) elevation of PKC-beta, Prex1 and Bik gene transcripts; (c) specific methylation decreases in the promoter region of Prex1; and (d) elevated phosphorylation of Rac1-Ser71, PKC-beta-Ser660, total PKC-beta, PKC-alpha-Ser657 and p66shc-Ser36. It is notable that the elevation of Bik was previously shown to correlate with oxidative stress.^{20,21} These results are consistent with and supportive of our main hypothesis.

In all cases except total PKC-beta and PKC-alpha protein and transcripts, treatment of burned animals with nephrlin reversed the effects of burn stress. Taken together with the array data, these results seem to implicate Rac1

activation in nephrilin's mechanism of action via Rictor complex. Additional studies will be needed to prove this point conclusively.

Rictor complex is implicated in the activation of Prex1, PKCs alpha and beta-2 and — indirectly through PKC-beta-2 — p66shc.^{12,18,26,27} Our results, taken together, suggest at least two pathways (PKC-beta and Prex1) through which Rictor complex might control the activation of Rac1/2, and possibly a third via activated PKC-alpha and ERK.²⁶ One may further speculate that Rictor (mTORC2) complex acts as a central regulator of oxidative metabolism in mammalian cells in response to stress and may even influence apoptosis through effectors like Bik. The documented pleiotropic protective effects of nephrilin peptide in numerous and diverse rodent models of metabolic, xenobiotic and traumatic stress.⁵⁻⁸ could thus be explained if the Rictor-controlled generation of oxidative stress via Rac1 and NADPH oxidase in these disease models amplifies the disease state (for example, by inducing elevated levels of ROS-triggered inflammation stress or Bik-triggered apoptosis).

Additionally, the effect of nephrilin treatment on the enduring effects of burn stress could be related to stress-triggered changes in epigenetic programs of histone modification and DNA methylation. As we show in this study, nephrilin treatment of animals reverses significant elevations in histone phosphorylation and acetylation as well as CpG methylation changes in the Prex1 promoter region. This observation, combined with our data showing substantial elevations of transcription for PKC-beta and Prex1 as well as total immunoreactive PKCs, and bearing in mind the role of these proteins in Rac1 activation leads us to speculate that perhaps the initial traumatic stress event generates persistent changes via epigenetic programs that affect gene expression levels and protein pools. Interestingly, methylation of Prex1 and PKC genes have previously been shown to affect gene transcription by others.^{28,29} Such transcriptionally-derived changes in 'set point' by increasing the steady state pool of protein could produce exaggerated responses to subsequent stressful stimuli when that pool of protein is post-translationally activated by phosphorylation, thereby setting the stage for a chronic feed-forward state. As Rictor complex regulates the activation of PKC-alpha, PKC-beta, p66shc and Prex1, inactivation of Rictor complex with its designed inhibitor nephrilin would (in theory) allow cells to exit this chronic feed-forward state, despite the presence of elevated PKC and Prex1 substrate pools. This, in turn, might allow a gradual return to the epigenetic baseline initially disrupted by the traumatic stress.

Further studies will be required to show the generality of nephrilin's protective effects on tissues other than kidney. Of particular interest to us is the possible effect of this agent on protecting the CNS, a known target of stress-related damage that can persist for a lifetime e.g. in PTSD and even, possibly, several lifetimes.¹⁻³

Acknowledgements

We thank Dr. Celeste Finnerty and Dr. Amina ElAyadi for their generous gift of frozen rat tissues used in this study. This work was supported in part by the Department of Pediatrics at the University of Mississippi Medical Center and the Bower Foundation.

Disclosure

The authors report no conflicts of interest in this work.

References

1. Exposome review: Bale TL. Lifetime stress experience: transgenerational epigenetics and germ cell programming. *Dialogues Clin Neurosci*. 2014 Sep;16(3):297–305.
2. Zucchi FC, Yao Y, Metz GA. The secret language of destiny: stress imprinting and transgenerational origins of disease. *Front Genet*. 2012 Jun 4;3:96.
3. Bowers ME, Yehuda R. Intergenerational Transmission of Stress in Humans. *Neuropsychopharmacology*. 2016 Jan;41(1):232–244.
4. Yehuda R, Daskalakis NP, Bierer LM, Bader HN, Klengel T, Holsboer F, Binder EB. Holocaust Exposure Induced Intergenerational Effects on FKBP5 Methylation. *Biol Psychiatry*. 2016 Sep 1;80(5):372–380.
5. Singh BK, Singh A, Mascarenhas DD. A nuclear complex of rictor and insulin receptor substrate-2 is associated with albuminuria in diabetic mice. *Metab Syndr Relat Disord*. 2010 Aug; 8(4): 355–363.
6. Mascarenhas D, Routt S, Singh BK. Mammalian target of rapamycin complex 2 regulates inflammatory response to stress. *Inflamm Res*. 2012 Dec; 61(12): 1395–1404.
7. Mascarenhas DD, El Ayadi A, Singh BK, Prasai A, Hegde SD, Herndon DN, Finnerty CC. Nephrilin peptide modulates a neuroimmune stress response in rodent models of burn trauma and sepsis. *Int J Burns Trauma*. 2013 Nov 1; 3(4): 190–200.
8. Mascarenhas DD, Ayadi AE, Wetzel M, Prasai A, Mifflin R, Jay J, Herndon DN, Finnerty CC. Effects of the nephrilin peptide on post-burn glycemic control, renal function, fat and lean body mass, and wound healing. *Int J Burns Trauma*. 2016 Nov 30;6(3):44–50.
9. Parat MO, Richard MJ, Leccia MT, Amblard P, Favier A, Beani JC. Does manganese protect cultured human skin fibroblasts against oxidative injury by UVA, dithranol and hydrogen peroxide? *Free Radic Res*. 1995 Oct;23(4):339–351.
10. Seité S, Colige A, Piquemal-Vivenot P, Montastier C, Fourtanier A, Lapière C, Nussgens B. A full-UV spectrum absorbing daily use cream protects human skin against biological changes occurring in photoaging. *Photodermatol Photoimmunol Photomed*. 2000 Aug;16(4):147–155.
11. Arany I, Faisal A, Clark JS, Vera T, Baliga R, Nagamine Y. p66SHC-mediated mitochondrial dysfunction in renal proximal tubule cells during oxidative injury. *Am J Physiol Renal Physiol*. 2010 May;298(5):F1214–21.
12. Pinton P, Rizzuto R. p66Shc, oxidative stress and aging: importing a lifespan determinant into mitochondria. *Cell Cycle*. 2008 Feb 1;7(3):304–308.

13. De Marchi E, Baldassari F, Bononi A, Wieckowski MR, Pinton P. Oxidative stress in cardiovascular diseases and obesity: role of p66Shc and protein kinase C. *Oxid Med Cell Longev*. 2013;2013:564961.
14. Herndon DN, Wilmore DW, Mason AD Jr. Development and analysis of a small animal model simulating the human postburn hypermetabolic response. *J Surg Res*. 1978 Nov;25(5):394–403.
15. Song J, Liu P, Yang Z, Li L, Su H, Lu N, Peng Z. MiR-155 Negatively Regulates c-Jun Expression at the Post-transcriptional Level in Human Dermal Fibroblasts in vitro: Implications in UVA Irradiation-induced Photoaging. *Cell Physiol Biochem*. 2012;29(3-4):331–340.
16. Arany I, Clark J, Reed DK, Juncos LA. Chronic nicotine exposure augments renal oxidative stress and injury through transcriptional activation of p66shc. *Nephrol Dial Transplant*. 2013 Jun;28(6):1417–1425.
17. Arany I, Hall S, Reed DK, Dixit M. The pro-oxidant gene p66shc increases nicotine exposure-induced lipotoxic oxidative stress in renal proximal tubule cells. *Mol Med Rep*. 2016 Sep;14(3):2771–2777.
18. Hernández-Negrete I, Carretero-Ortega J, Rosenfeldt H, Hernández-García R, Calderón-Salinas JV, Reyes-Cruz G, Gutkind JS, Vázquez-Prado J. P-Rex1 links mammalian target of rapamycin signaling to Rac activation and cell migration. *J Biol Chem*. 2007 Aug 10;282(32):23708–23715.
19. Welch HC. Regulation and function of P-Rex family Rac-GEFs. *Small GTPases*. 2015;6(2):49–70.
20. Trejo-Vargas A, Hernández-Mercado E, Ordóñez-Razo RM, Lazzarini R, Arenas-Aranda DJ, Gutiérrez-Ruiz MC, Königsberg M, Luna-López A. Bik subcellular localization in response to oxidative stress induced by chemotherapy, in two different breast cancer cell lines and a non-tumorigenic epithelial cell line. *J Appl Toxicol*. 2015 Nov;35(11):1262–1270.
21. Bodet L, Ménoret E, Descamps G, Pellat-Deceunynck C, Bataille R, Le Gouill S, Moreau P, Amiot M, Gomez-Bougie P. BH3-only protein Bik is involved in both apoptosis induction and sensitivity to oxidative stress in multiple myeloma. *Br J Cancer*. 2010 Dec 7;103(12):1808–1814.
22. Huang W, Mishra V, Batra S, Dillon I, Mehta KD. Phorbol ester promotes histone H3-Ser10 phosphorylation at the LDL receptor promoter in a protein kinase C-dependent manner. *J Lipid Res*. 2004 Aug;45(8):1519–1527.
23. Sharma AK, Mansukh A, Varma A, Gadewal N, Gupta S. Molecular Modeling of Differentially Phosphorylated Serine 10 and Acetylated lysine 9/14 of Histone H3 Regulates their Interactions with 14-3-3 ζ , MSK1, and MKP1. *Bioinform Biol Insights*. 2013 Aug 26;7:271–288.
24. Ohashi N, Urushihara M, Kobori H. Activated intrarenal reactive oxygen species and renin angiotensin system in IgA nephropathy. *Minerva Urol Nefrol*. 2009 Mar;61(1):55–66.
25. Del Ben M, Fabiani M, Loffredo L, Polimeni L, Carnevale R, Baratta F, Brunori M, Albanese F, Augelletti T, Violi F, Angelico F. Oxidative stress mediated arterial dysfunction in patients with obstructive sleep apnoea and the effect of continuous positive airway pressure treatment. *BMC Pulm Med*. 2012 Jul 23;12:36.
26. Kumar A, Chambers TC, Cloud-Heflin BA, Mehta KD. Phorbol ester-induced low density lipoprotein receptor gene expression in HepG2 cells involves protein kinase C-mediated p42/44 MAP kinase activation. *J Lipid Res*. 1997 Nov;38(11):2240–2248.
27. Kirmani D, Bhat HF, Bashir M, Zargar MA, Khanday FA. P66Shc-rac1 pathway-mediated ROS production and cell migration is downregulated by ascorbic acid. *J Recept Signal Transduct Res*. 2013 Apr; 33(2):107–113.
28. Barrio-Real L, Benedetti LG, Engel N, Tu Y, Cho S, Sukumar S, Kazanietz MG. Subtype-specific overexpression of the Rac-GEF P-REX1 in breast cancer is associated with promoter hypomethylation. *Breast Cancer Res*. 2014 Sep 24;16(5):441.
29. Hagiwara K, Ito H, Murate T, Miyata Y, Ohashi H, Nagai H. PROX1 overexpression inhibits protein kinase C beta II transcription through promoter DNA methylation. *Genes Chromosomes Cancer*. 2012 Nov;51(11):1024–1036.

Biologics: Targets and Therapy

Publish your work in this journal

Biologics: Targets and Therapy is an international, peer-reviewed journal focusing on the patho-physiological rationale for and clinical application of Biologic agents in the management of autoimmune diseases, cancers or other pathologies where a molecular target can be identified. This journal is indexed on PubMed Central, EMBase, and Scopus.

Submit your manuscript here: <https://www.dovepress.com/biologics-targets-and-therapy-journal>

Dovepress

The manuscript management system is completely online and includes a very quick and fair peer-review system, which is all easy to use. Visit <http://www.dovepress.com/testimonials.php> to read real quotes from published authors.